A coupled parametric and nonparametric approach for modal analysis of a satellite.

S. Dubreuil
Centre National d'Études Spatiales (CNES), Toulouse, France

F. Petitjean
Institut Catholique d'Arts et Métiers (ICAM), Toulouse, France

M. Salaün
ISAE-Institut Clément Ader (ICA), Toulouse, France

ABSTRACT: This study takes place in the context of dynamical prediction for satellite structures. Aims of such studies are to survey the dynamical response of satellite equipment and components, to check that requirements are correct and to give prediction of vibration levels, which are inputs for the experimental test validation according to the launcher specification. This prediction is done by modal analysis performed on a numerical model built by finite element method. Uncertainties on equipment and components properties lead to random frequency response function (FRF). This paper aims at understanding how modal approach can be adapted to probabilistic framework in order to calculate cumulative density function or, at least, some quantiles of a FRF. Starting point of deterministic modal analysis is the study of a single degree of freedom (DOF) system. C. Heinkelé analytically expresses the probability density function (PDF) of the FRF of an oscillator with a random natural pulsation following a uniform law. We have generalized this work to random natural pulsation following a law of finite variance. Then, the expression of a FRF between two DOF of the structure is a linear function of random oscillators FRF and DOF components of random eigenvectors. Assuming that random eigenvectors are close to their means, we have access to the characteristic function of the random FRF between two DOF as a multi-dimensional integral with respect to the joint PDF of the oscillators FRF. This paper mainly focuses on two major points which are calculation of oscillators joint PDF and inversion of characteristic functions. The first one is tackled by copulas theory. Dependence structure of random eigenvalues are identified and modeled by a copula. Then we apply results on copulas transformations to obtain joint PDF of oscillators FRF. Classical results concern monotonic transformations but we extended these ones to non-monotonic cases. Concerning inversion of characteristic function, several methods are studied to numerically compute the Gil-Pelaez formula. This approach allows to access some FRF quantiles by numerical integration which error can be controlled. Moreover, an interesting point is the flexibility in the identification of the random eigenvalues PDF. This is especially interesting in order to couple parametric identification with nonparametric one, when only few dispersion informations are given for equipments, housed in the satellite primary structure.

1 OSCILLATOR WITH RANDOM NATURAL PULSATION

Starting point of modal analysis is the single DOF system. In deterministic context its transfer function is

$$H(\omega) = \frac{-\omega^2 + \underline{\lambda}}{(-\omega^2 + \underline{\lambda})^2 + 4\xi\underline{\lambda}\omega^2} + j\frac{-2\xi\sqrt{\underline{\lambda}}\omega}{(-\omega^2 + \underline{\lambda})^2 + 4\xi\underline{\lambda}\omega^2}$$

where $j^2 = -1$, ω is the pulsation, ξ the critical damping coefficient and $\underline{\lambda}$ the square of the natural deterministic pulsation. Uncertainties on oscillator properties (stiffness, mass) lead to random natural pulsation. Let λ be the random variable modeling the square of random natural pulsation, p_λ its PDF and $H(\omega)$ the associated transfer function. Following results presented in (Heinkelé 2008), we calculate PDF of transfer function presented above (difference with the work in (Heinkelé 2008) is critical damping model and generalization to λ a second order random variable). As methodology for real, imaginary part or module and phase is similar, we illustrate our study on

real part of transfer function, which expression reads

$$\begin{aligned} \mathcal{F} : \mathbb{R} &\to \left[\frac{1}{4\xi\omega^2\,(\xi-1)} ; \frac{1}{4\xi\omega^2\,(\xi+1)} \right] \\ \mathcal{F}(\lambda;\xi,\omega) = Re(H) &= \frac{-\omega^2+\lambda}{(-\omega^2+\lambda)^2+4\xi^2\lambda\omega^2} \end{aligned} \tag{1}$$

It should be noted that this transformation is non-monotonic and have two inverse images called $\mathcal{F}_1^{-1}$, $\mathcal{F}_2^{-1}$. Then, one can expresses PDF of $Re(H(\omega))$ using classical results on random variable transformations. This leads to:

$$\begin{aligned} p_{Re(H)}(Re(h)) &= \frac{p_\lambda(\mathcal{F}_1^{-1}(Re(h)))}{|J_{Re}(\mathcal{F}_1^{-1}(Re(h)))|} \\ &+ \frac{p_\lambda(\mathcal{F}_2^{-1}(Re(h)))}{|J_{Re}(\mathcal{F}_2^{-1}(Re(h)))|} \end{aligned} \tag{2}$$

where J_{Re} is the jacobian of transformation (1). Integration of this density is possible since λ follows a second order probability law, which is an acceptable assumption in our context. Numerical integration of this PDF allows to access mean, standard deviation, and quantiles of $Re(H)$. Figure 1 shows various shapes of this function for different ω values when p_λ follows a normal law.

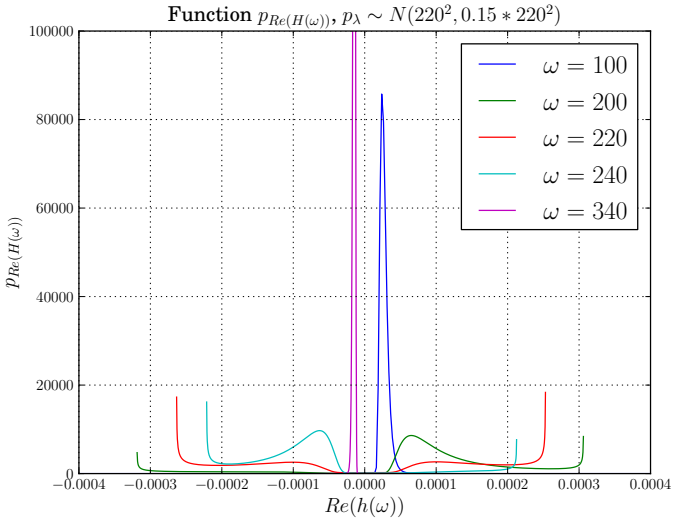

Figure 1: Shape of the density $p_{Re(H)}(Re(h))$ when p_λ follows a normal law.

Two difficulties arise during numerical integration. First one is the infinite limit at edges of domain. This problem is solved by using numerical integration on $[\frac{1-\epsilon}{4\xi\omega^2\,(\xi-1)}, \frac{1-\epsilon}{4\xi\omega^2\,(\xi+1)}]$ and by analytical integration of an equivalent of the density on $[\frac{1}{4\xi\omega^2\,(\xi-1)}, \frac{1-\epsilon}{4\omega^2\,(\xi-1)}]$ and $[\frac{1-\epsilon}{4\xi\omega^2\,(\xi+1)}, \frac{1}{4\xi\omega^2\,(\xi+1)}]$. Second one concerns the shape of the density when ω is far from $\sqrt{E[\lambda]}$. As it can be seen on figure 1 for $\omega = 100$ and $\omega = 340$ the density looks like a single peak with a very strong slope. In fact, density tends to a zero Dirac distribution. Thus, to have a correct numerical integration, discretization of the density must be done according to its derivative.

Figure 2 shows results of this methodology in determination of 2.5%, 50% and 97.5% quantiles in comparison with Monte-Carlo method (one million runs).

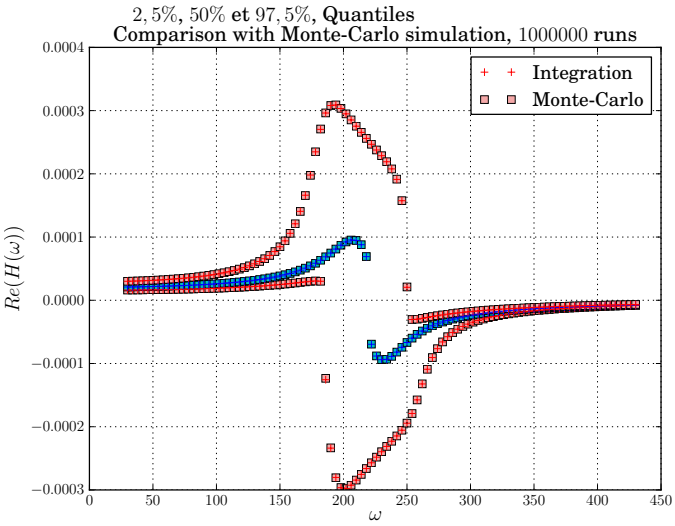

Figure 2: Determination of the 2.5%, 50% and 97.5% quantiles by integration and comparison with Monte-Carlo simulations, p_λ follows a normal law.

Numerical integration on regular domain is performed by trapezoidal rule, number of points depends on the pulsation ω, for reasons explained previously. Results presented by figure 2 allow to be confident in this integration methodology.

In order to adapt deterministic modal analysis to probabilistic framework, we now present a generalization of these results to a multi-degree of freedom system.

2 ADAPTATION TO MULTI DOF

2.1 *Modal synthesis*

Let us consider a finite element model of a mechanical structure. We denote $[\underline{\underline{M}}]$, $[\underline{\underline{K}}]$, $[\underline{\underline{D}}]$ the mass, stiffness and damping matrices of the mean model (model for which input parameters are set to their means). In frequency domain, vibration equation reads

$$\left(-\omega^2\,[\underline{\underline{M}}] + j\omega\,[\underline{\underline{D}}] + [\underline{\underline{K}}]\right)\underline{y}(\omega) = \underline{f}(\omega)$$

in which $\underline{y}(\omega)$ is the vector of the DOF and $\underline{f}(\omega)$ is the vector of loads input to the system. Modal synthesis is based on solving following eigenvalues problem

$$\left(-\omega^2\,[\underline{\underline{M}}] + [\underline{\underline{K}}]\right)\underline{y} = 0.$$

Aims of modal analysis is to select a basis $[\underline{\underline{\varphi}}]$ of eigenvectors which dimension N is far less from the number of DOF. We denote by $\underline{\lambda}_k, k = 1 \cdots N$, corresponding eigenvalues. This approach relies on assumption that low frequency comportment of structure can be expressed on a reduced basis composed

by first eigenvectors. In this basis, mass and stiffness matrices are diagonal and a current assumption is to consider that the damping one is diagonal too. This leads to a diagonal transfer functions matrix

$$[\underline{H}]_{kk}(\omega) = \frac{-\omega^2 + \underline{\lambda_k}}{(-\omega^2 + \underline{\lambda_k})^2 + 4\xi_k \underline{\lambda_k} \omega^2} + j \frac{-2\xi_k \sqrt{\underline{\lambda_k}}\omega}{(-\omega^2 + \underline{\lambda_k})^2 + 4\xi_k \underline{\lambda_k} \omega^2}$$

which is an oscillator equation described in the first part. Then, FRF between two DOF a and b of a structure is: $[\underline{F}]_{ab} = \sum_{i=1}^{N} [\underline{H}]_{ii} [\underline{\varphi}]_{bi} [\underline{\varphi}]_{ai}$.

Uncertainties on input parameters leads to a random eigenvalues problem. At this step, we assume that the random eigenvector basis is close to the deterministic basis $[\underline{\varphi}]$. Random transfer matrix $[\mathbf{H}]$ is diagonal and each term is a random oscillator studied in first part. Let us call $Re(\{\mathbf{H}\})$ the random vector composed by real part of diagonal terms of $[\mathbf{H}]$. As transformation giving FRF between two DOF a and b of a structure is a linear combination between terms of the random vector $Re(\{\mathbf{H}\})$, one obtains the characteristic function of $Re(F_{ab})$.

$$\Phi_{Re(F_{ab})}(v) = \int_{\mathbb{R}^N} \exp(jv \sum_{i=1}^{N} Re(h_i)[\underline{\varphi}]_{bi}[\underline{\varphi}]_{ai}) \; p_{Re(\{\mathbf{H}\})}(Re(\{\mathbf{h}\}))\mathrm{d}Re(\{\mathbf{h}\}) \quad (3)$$

Once calculation of this characteristic function is done, inversion formulas like Gil-Pelaez one (Gil-Pelaez 1951) or Poisson summation (Abate and Whitt 1992) allows to access CDF or PDF of $Re(F_{ab})$. As equation (3) is a multi dimensional integral respectively to the joint density of $Re(\{\mathbf{H}\})$, it is of great importance to study dependence structure of this random vector.

2.2 *Independant case*

The simplest assumption is to consider that random variables $Re(H_k)$ for $k = 1, \cdots, N$, of $Re(\{\mathbf{H}\})$ are independent and of marginal density described in the first section. Then, equation (3) becomes a product of N integrals in one dimension

$$\Phi_{Re(F_{ab})}(v) = \prod_{i=1}^{N} \int \exp(jv[\underline{\varphi}]_{bi}[\underline{\varphi}]_{ai} Re(h_i)) \; p_{Re(H_i)}(Re(h_i))\mathrm{d}Re(h_i),$$

which leads to

$$\Phi_{Re(F_{ab})}(v) = \prod_{i=1}^{n} \frac{1}{|[\underline{\varphi}]_{bi}[\underline{\varphi}]_{ai}|} \Phi_{Re(H_i)}(v)$$

with an appropriate change of variable.

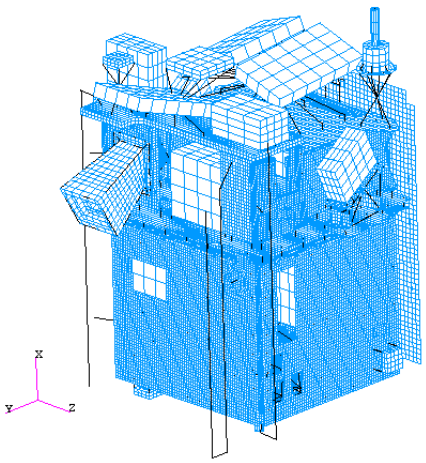

Figure 3: Finite element model of TARANIS satellite.

Nevertheless, assumption of independent eigenvalues seems unrealistic. For example, let us introduce the finite element model of satellite TARANIS presented by figure 3.

Input properties of this structure are modeled by independent random variables (input properties are materials ones like Young modulus and Poisson coefficient and geometric ones like thickness of panels etc.). Figure 4 presents dispersion of the two first eigenvalues coming from 1000 runs of this random model. It is clear that these two random eigenvalues are correlated, so modeling and consequence on FRF of this correlation must be investigated.

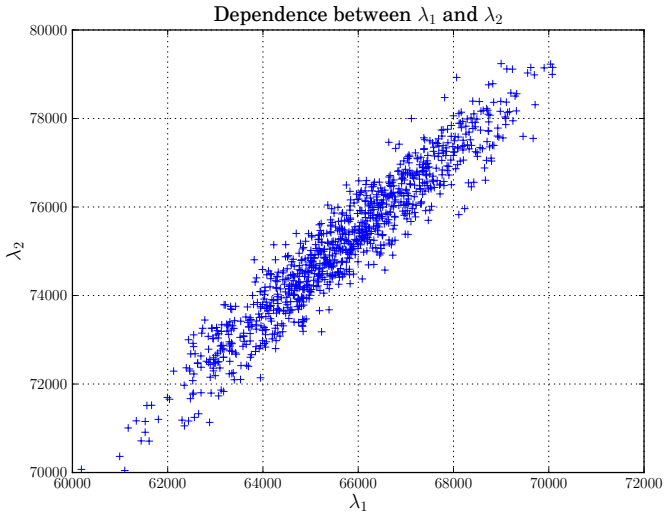

Figure 4: Two first eigenvalues of TARANIS model, 1000 runs.

2.3 *Dependence model*

In this part, we set $N = 2$ in order to simplify expressions but generalization is straightforward. Moreover, in practice the case $N = 2$ should be frequent as correlation of eigenvalues needs to be modeled only if oscillators are acting on same pulsations range. We are interested in modeling the joint probability law of random vector $Re(\{\mathbf{H}\})$ whose marginal laws are described in previous section. To build this model we

propose to use copulas theory introduced in (Nelsen 2006) and (Clauss). Indeed, a result known as Sklar theorem allows to build joint PDF of random eigenvalues, and to express it as,

$$p_{\lambda_1,\lambda_2}(\lambda_1,\lambda_2) = p_{\lambda_1}(\lambda_1)p_{\lambda_2}(\lambda_2)c(F_{\lambda_1}(\lambda_1),F_{\lambda_2}(\lambda_2))$$

where c is the density of the copula modeling the dependence structure of eigenvalues and F_i the marginal CDF of λ_i. In order to express joint density of $Re(\{\mathbf{H}\})$, we use results on random variable transformation and copula transformation presented in (Nelsen 2006). These last ones are derived for monotonic transformation. Non monotonic application presented here is the principal difficulty.

Let Λ be the random vector $[\lambda_1,\lambda_2]$ of joint density $p_{\lambda_1,\lambda_2}(\lambda_1,\lambda_2)$ described above and f the function of $\mathbb{R}^2$ with values in $\left[\frac{1}{4\xi_1\omega^2(\xi_1-1)}\,;\frac{1}{4\xi_1\omega^2(\xi_1+1)}\right]\times\left[\frac{1}{4\xi_2\omega^2(\xi_2-1)}\,;\frac{1}{4\xi_2\omega^2(\xi_2+1)}\right]$.

$$f\begin{pmatrix}\lambda_1\\ \lambda_2\end{pmatrix} = \begin{pmatrix} Re(H_1)=\mathcal{F}(\lambda_1\,;\xi_1,\omega)\\ Re(H_2)=\mathcal{F}(\lambda_2\,;\xi_2,\omega)\end{pmatrix}$$

where $\mathcal{F}$ is the function described by equation (1). Finally, one accesses density of $Re(\{\mathbf{H}\})$ in function of previous transformation, marginal density of eigenvalues and copula modeling dependence structure of eigenvalues:

$$\begin{aligned}&p_{Re(\{\mathbf{H}\})}(Re(\{\mathbf{h}\})) =\\ &\sum_{i,j=1}^{2}\left[\frac{p_{\lambda_1}(\mathcal{F}_i^{-1}(Re(H_1)))}{|J(\mathcal{F}_i^{-1}(Re(H_1)))|}\times\frac{p_{\lambda_2}(\mathcal{F}_j^{-1}(Re(H_2)))}{|J(\mathcal{F}_j^{-1}(Re(H_2)))|}\times\right.\\ &\left.c\left(F_1(\mathcal{F}_i^{-1}(Re(H_1))),F_2(\mathcal{F}_j^{-1}(Re(H_2)))\right)\right]\end{aligned} \tag{4}$$

This density is used to numerically calculate the characteristic function (3).

3 NUMERICAL RESULTS

3.1 *Dependence structure of* $Re(\{\boldsymbol{H}\})$

In order to illustrate our methodology, we propose to consider two random oscillators with dependent random eigenvalues :

- λ_1 follows a normal law of mean 220^2 and a variation coefficient of 15%.
- λ_2 follows a triangular law defines on $[50000, 75000]$ with a maximum at 59375
- Eigenvalues dependence is modeled by a normal copula of Kendall correlation coefficient equal to 0.95.

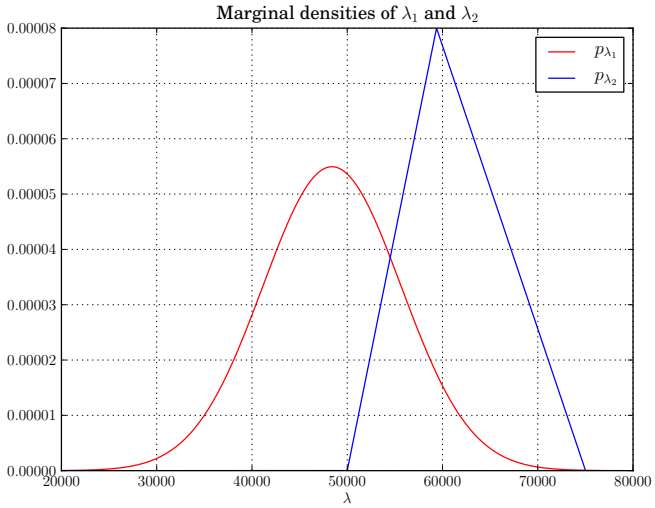

Figure 5: Marginal densities p_{λ_1}, p_{λ_1}.

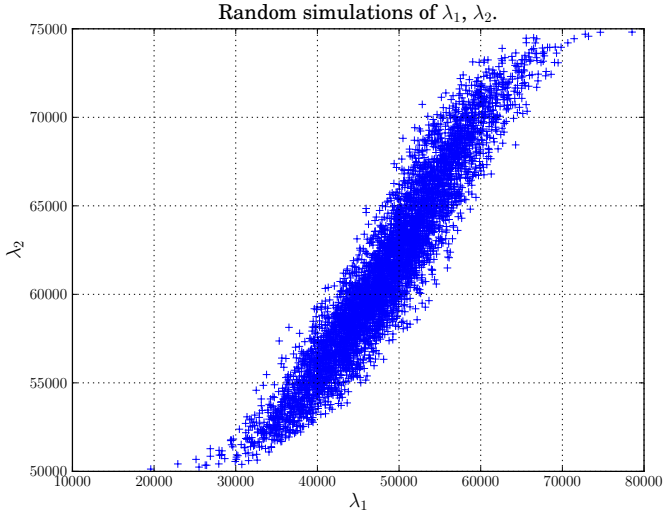

Figure 6: Random simulation of λ_1, λ_2 following joint density p_{λ_1,λ_2}.

Figure 5 shows shapes of marginal densities of λ_1 and λ_2 and figure 6 illustrates joint density of eigenvalues.

Note that in an industrial application uncertainties come from input parameters of model, then construction of eigenvalues stochastic model have to be done by identification. This part is not developed here but several tools are available in order to identified marginal densities and copula.

Once probabilistic model of eigenvalues is built, we are interested in representation of the joint density of random vector $Re(\{\mathbf{H}\})$.

In order to compare an empirical density of $Re(\{\mathbf{H}\})$ to the one obtained by our method, we run a Monte-Carlo simulations at a pulsation $\omega = 235\ rad.s^{-1}$ from a sample of 5000 eigenvalues λ_1, λ_2 drawn in p_{λ_1,λ_2}. Results of these simulations is presented by figure 7.

Density obtained from the expression (4) is presented by figure 8.

Influence of correlation of eigenvalues is illustrated by figure 9 which is a simulation of the joint PDF of $Re(\{\mathbf{H}\})$ if we consider independent eigenvalues.

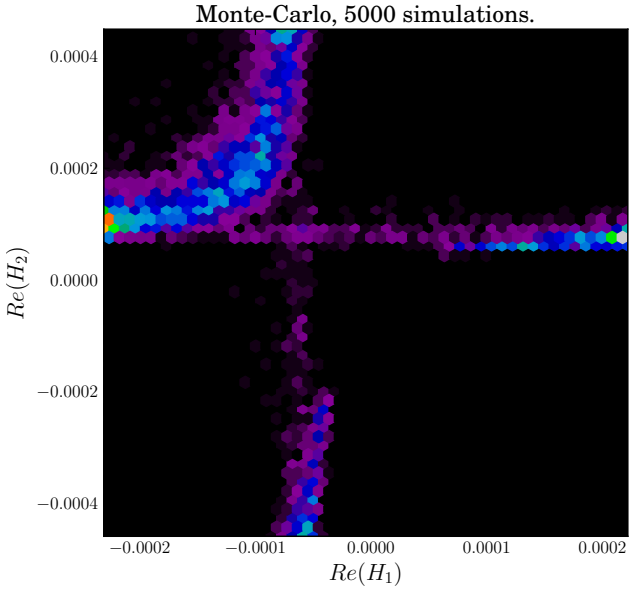

Figure 7: Random simulations of $Re(\{\mathbf{H}\})$, at $\omega = 235\ rad.s^{-1}$.

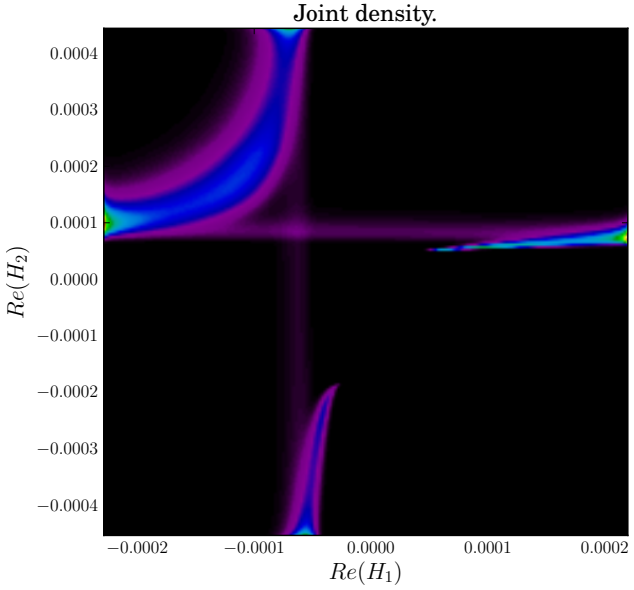

Figure 8: Simulation of the density of $Re(\{\mathbf{H}\})$, at $\omega = 235 rad.s^{-1}$.

It appears clearly that correlation of eigenvalues strongly influence joint PDF of $Re(\{\mathbf{H}\})$. Moreover, empirical joint PDF of $Re(\{\mathbf{H}\})$ (figure 7) seems really close to simulated one (figure 8) which confirms capability of analytical formulation based on copula transformation.

As we can now express analytically joint PDF of $Re(\{\mathbf{H}\})$, knowing eigenvalues stochastic model, we use it to numerically compute the characteristic function (3).

3.2 *Computation of the real part FRF CDF*

For illustrating our methodology we consider $[\underline{\varphi}]_{bi} = [\underline{\varphi}]_{ai} = 1$ and then we compute the characteristic function (3). Numerical integration of dimension two (equation (3)) is performed on the domain $[\frac{1-\epsilon}{4\xi_1\omega^2\,(\xi_1-1)}, \frac{1-\epsilon}{4\xi_1\omega^2\,(\xi_1+1)}] \times [\frac{1-\epsilon}{4\xi_2\omega^2\,(\xi_2-1)}, \frac{1-\epsilon}{4\xi_2\omega^2\,(\xi_2+1)}]$.

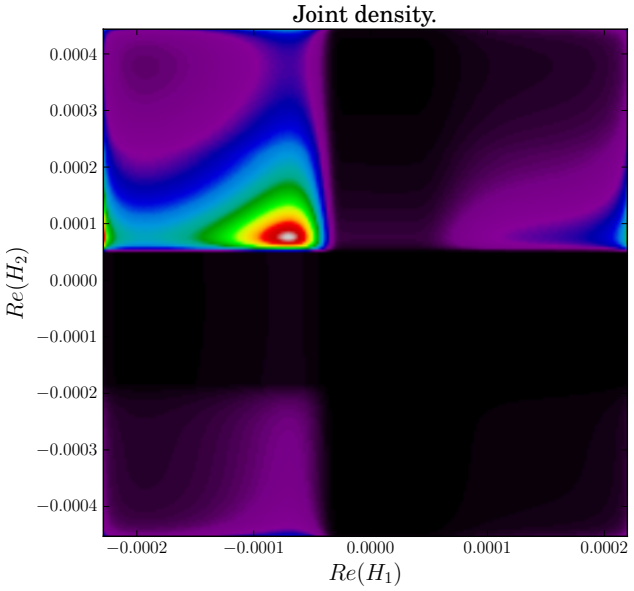

Figure 9: Simulation of the density of $Re(\{\mathbf{H}\})$, at $\omega = 235 rad.s^{-1}$, with independent eigenvalues.

This domain is meshed by quadrangles which are tensorial product of marginal p_{λ_1}, p_{λ_2} discretizations (according to differential of marginal).

In the following F_{ab} stands for real part of random FRF between two DOF a and b and f_{ab} for one sample. Once characteristic function is computed, several post treatments can be performed. First of all, Gil-Pelaez formula (Gil-Pelaez 1951) is used to access the CDF of F_{ab} and this formula gives

$$P[F_{ab} < f_{ab}] = \frac{1}{2} - \frac{1}{\pi}\int_0^\infty \frac{Im[e^{-jf_{ab}v}\Phi_{Re(F_{ab})}(v)]}{v}\mathrm{d}v$$

In order to compute this integral, we use the method described by Davies (Davies 1973) based on Fourier cosine series summation formula.

$$P[F_{ab} < f_{ab}] = \frac{1}{2} - \sum_{k=0}^{K} \frac{Im\left[\Phi_{Re(F_{ab})}((k+0.5)h)e^{-j(k+0.5)hf_{ab}}\right]}{\pi(k+0.5)}\ .$$

The author recommends to choose a discretization step h, for which $max\left\{P(F_{ab} < f_{ab} - \frac{2\pi}{h})\ ,\ P(F_{ab} > f_{ab} + \frac{2\pi}{h})\right\}$ is less than half the maximum allowable error. In our application F_{ab} is bounded and $f_{ab} \in [B_1, B_2]$ with $B_1 = \frac{[\varphi]_{a1}[\varphi]_{b1}}{4\xi_1\omega^2(\xi_1-1)} + \frac{[\varphi]_{a2}[\varphi]_{b2}}{4\xi_2\omega^2(\xi_2-1)}$ and $B_2 = \frac{[\varphi]_{a1}[\varphi]_{b1}}{4\xi_1\omega^2(\xi_1+1)} + \frac{[\varphi]_{a2}[\varphi]_{b2}}{4\xi_2\omega^2(\xi_2+1)}$. Then it follows that $P(F_{ab} > B_1 + \frac{2\pi}{h}) = 0 \Leftrightarrow B_1 + \frac{2\pi}{h} > B_2 \Leftrightarrow h < \frac{2\pi}{B_2 - B_1}$.

As series converge fast to zero, truncation until the K term is done when $\Phi_{Re(F_{ab})}((K+0.5)h) = 0 + \epsilon$.

Applying this methodology to the previous example and still considering $\omega = 235\ rad.s^{-1}$, the figure 10 illustrates CDF of F_{ab}. Comparison is done between Monte-Carlo method (one million runs), and

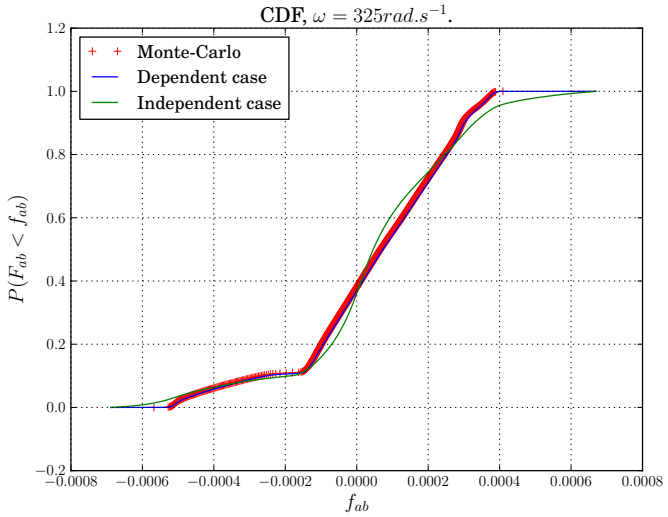

Figure 10: Comparison between CDF of F_{ab} obtained by Monte-Carlo method (red cross) and Gil-Pelaez formula, taking into account correlation of eigenvalues (blue curve) or not (green curve), at $\omega = 235\ rad.s^{-1}$.

Gil-Pelaez formula considering or not dependence of eigenvalues.

Some conclusions can be drawn from this figure. Firstly, eigenvalues dependence structure must be considered to avoid strong differences in CDF of FRF between two DOF. Secondly, comparison with Monte-Carlo allows to be confident in integration methodology described above. Finally, these conclusions are reinforced by providing the corresponding PDF. This one (figure 11) is computed by Poisson summation formula (Abate and Whitt 1992) which is in this case $p_{F_{ab}}(f_{ab}) \approx \frac{h}{\pi} \sum_{k=0}^{K} \Phi_{Re(F_{ab})}(kh) \exp(-jkhf_{ab})$.

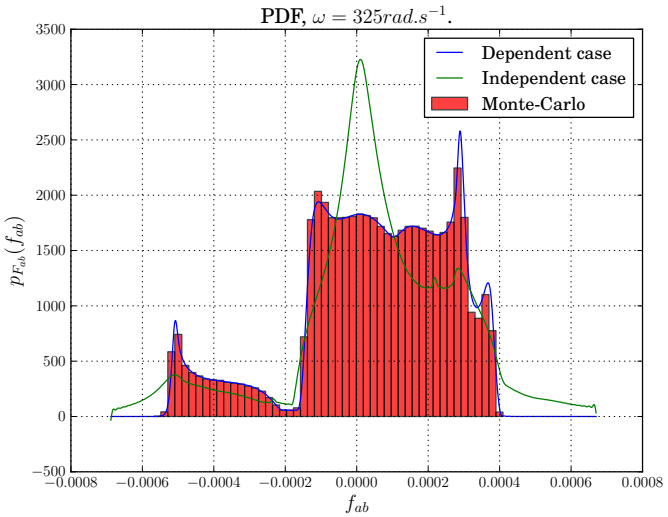

Figure 11: Comparison between PDF of F_{ab} obtained by Monte-Carlo method (red histogram) and Gil-Pelaez formula, taking into account correlation of eigenvalues (blue curve) or not (green curve), at $\omega = 235\ rad.s^{-1}$.

In previous example, ω is fixed to 235 $rad.s^{-1}$ which is a value between the two oscillators deterministic natural pulsation. First section of this paper shows that marginal eigenvalues densities are strongly influence by value pulsation, ω. Then, we illustrate the methodology on a range of pulsation. Considering the same example and looking for 2.5%, 50%, 97.5% quantiles of F_{ab}, previous methodology is applied and compared with Monte-Carlo method (100000 runs) on the pulsation range $[180 - 290] rad.s^{-1}$. Figure 12 presents the results.

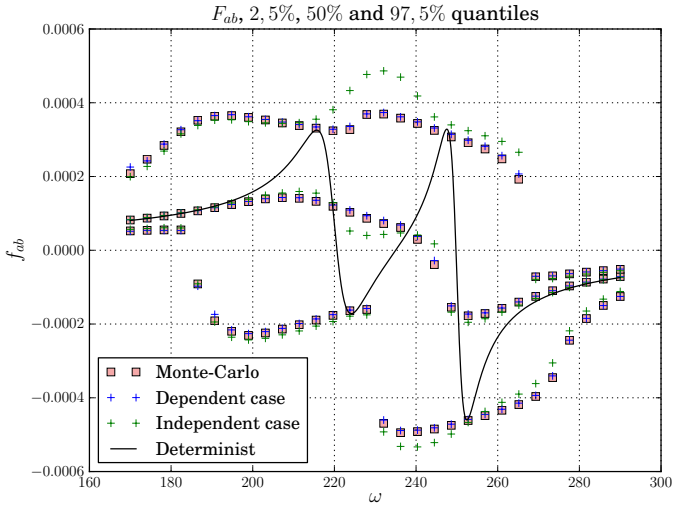

Figure 12: Determination of 2.5%, 50%, 97.5% quantiles of F_{ab}, comparison between Monte-Carlo (pink square) and Gil-Pelaez formula, taking into account correlation of eigenvalues (blue curve) or not (green curve).

As for previous results, comparison with Monte-Carlo method confirms capability of the two dimensional integration method. Moreover, it is interesting to see that this capability is conserved even at pulsation for which low variation of the FRF occurs. Influence of eigenvalues correlation clearly appears for 50% and 97.5% quantiles. For 97.5% quantiles, independent case reveals a single peak around $\omega = 230\ rad.s^{-1}$, which is not present in the dependent case.

All these numerical examples illustrates that correlation between eigenvalues strongly influence probability law of a FRF between two DOF. In addition, they show that copula is a suited tool to describe joint PDF of eigenvalues and then has to be used in determination of FRF CDF. Finally, integration method set-up in this context allows to consider that computation of the FRF CDF is performed with a negligible error.

This methodology is now applied to the satellite TARANIS (figure 3).

4 INDUSTRIAL APPLICATION : TARANIS

We consider the finite element satellite structure TARANIS previously introduced in part 2.2. More precisely, we investigate a particular FRF which deterministic value is drawn on figure 13.

This FRF is particularly interesting to apply our methodology as the two first modes of the structure

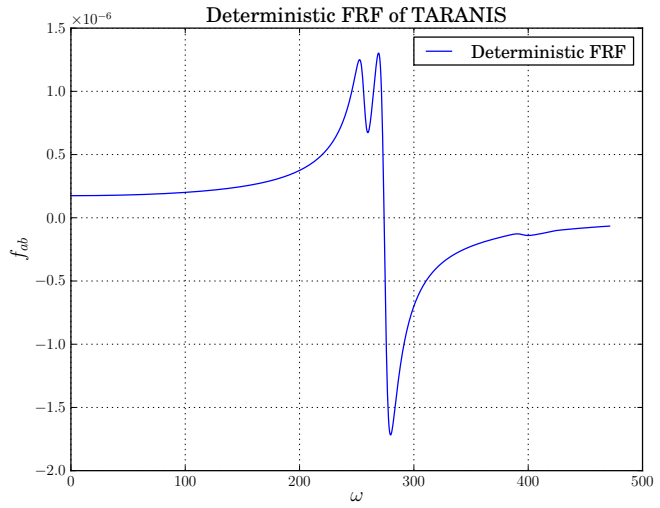

Figure 13: Deterministic FRF study in TARANIS example.

are stimulated and have very close natural pulsation.

As it have been told in part 3.1, in industrial applications uncertainties affect input parameters of the model. Without detailing this modelisation, parameters concerned in this example are Young modulus, Poisson ratio, panel thickness etc. Then, eigenvalues densities and correlation must be identified. In this example, we use a nonparametric identification by kernel smoothing over 100 realisation to get p_{λ_1} and p_{λ_2}. It is assumed that dependence structure is normal. Figure 14 shows the Kendall plot between the one hundred sample and the normal copula used to model dependence (Kendall plot is equivalent to quantiles-quantiles plot in two dimension, informations can be found in (Clauss) or (OpenTURNS 2011)). This

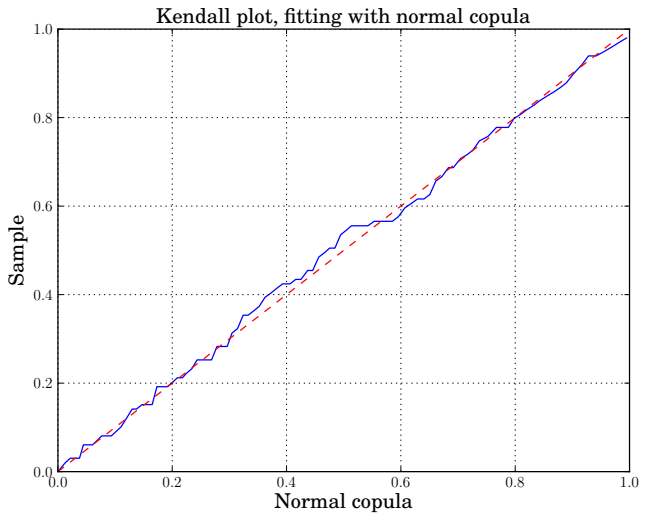

Figure 14: Kendall plot of the two first eigenvalues fitted by a normal copula.

curve shows that normal copula seems to be correct to model dependence between the two first eigenvalues.

Once identification process is done, one can applies the previous methodology. As above, we compute the 2.5%, 50%, 97.5% quantiles of the real part FRF. In order to have reference results, a Monte-Carlo simulation of 1000 runs is also performed and used to compute the 50% quantile. Note that, in this case, Monte-Carlo methodology consists in solving 1000 eigenvalues problems and compute corresponding FRF. Figure 15 presents the results. Reminding assumptions

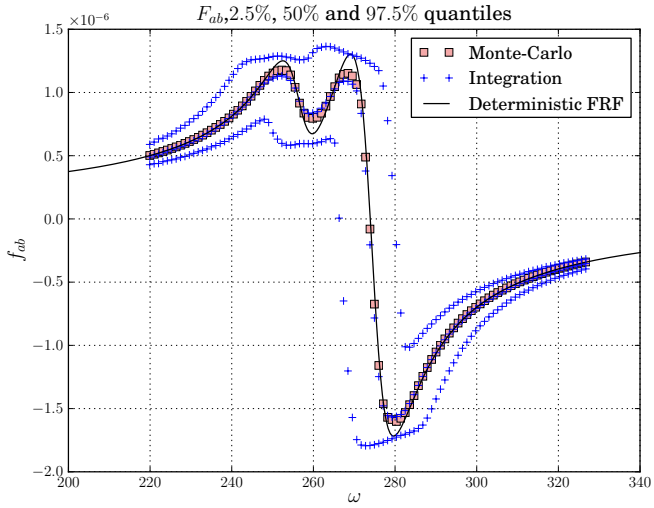

Figure 15: Determination of 2.5%, 50%, 97.5% quantiles, comparison with Monte-Carlo (1000 runs) for the 50% quantile.

done in the presented methodology, figure 15 illustrates errors due to deterministic eigenvector basis and identification of eigenvalues joint PDF. It clearly appears (in comparison with Monte-Carlo results) that this error is almost negligible. The 2.5% and 97.5% quantiles shapes seems relevant but we cannot confirm these results with only 1000 Monte-Carlo runs. Finally, this industrial example shows that identification of eigenvalues joint PDF is realistic and leads to relevant results.

5 CONCLUSION

Aims of this study was to present a method of probabilistic modal synthesis based on analytical expressions of the random oscillator PDF. All this article focuses on the importance of correlation between eigenvalues. First of all, modeling of eigenvalues dependence structure is performed by copula. Then we show how to use it in the determination of the joint PDF of the random vector of frequency response function $Re(\{\mathbf{H}\})$. Next, this joint PDF is used to determine the characteristic function of a frequency response function between two DOF and several solutions to numerically compute and make use of it are presented. At each step of this methodology, effect of correlation between eigenvalues is illustrated through a two dimensional example in part 3. These illustrations allow to draw two conclusions. First, the effect of correlation is non negligible and strongly affect the PDF of a FRF between two DOF of the system. Second, comparison with Monte-Carlo simulations confirms that integration methodology is rel-

evant and leads to a really good approximation of the PDF. Finally, an industrial application on Taranis satellite shows that eigenvalues joint PDF identification is realistic and allows to access some quantiles of the PDF FRF. Moreover, as it has been mentioned in introduction, this identification may be parametric, like in example part 3, or nonparametric, like in Taranis example (kernel smoothing). This is an advantage when only few information are available on eigenvalues variations (for example for some equipments housed in the satellite).

Perspectives for this work are to continue analytical process in the exploitation of copula properties (determination of frequency boundaries in which correlation have to be modeled). Then, we shall apply this methodology in a sub-structured model for which eigenvalues joint PDF of some sub-structures comes from nonparametric random matrices model such as the ones proposed by (Soize 2000) or (Adhikary et al. 2011).

ACKNOWLEDGMENTS

This work is supported by Centre National dÉtudes Spatiales (CNES) and Thales Alenia Space (TAS). The authors thank Fabrice Buffe (CNES), Jérôme Buffe and Anne Carpine (TAS).

REFERENCES

Abate, J. & W. Whitt (1992). The Fourier-series method for inverting transforms of probability distributions. *Queueing Systems 10*, 5–88.

Adhikary, S., L. Pastur, A. Lytova, & J. D. Bois (2011). Eigenvalue density of linear stochastic dynamical systems: Arandom matrix approach. *Jounal of Sound and Vibration 331*, 1042–1058.

Clauss, P. Théorie des copules. Notes de cours, ENSAI.

Davies, R. B. (1973). Numerical inversion of a characteristic function. *Biometrika 60*, 415–417.

Gil-Pelaez, J. (1951). Note on the inversion theorem. *Biometrika 38*, 481–483.

Heinkelé, C. (2008). *Synthèse modale probabiliste. Théorie et applications*. Ph. D. thesis, Université Claude Bernard-Lyon I, Lyon.

Nelsen, R. (2006). *An introduction to copulas*. Springer.

OpenTURNS (2011). *OpenTURNS : Reference Guide, V.0.15*. `http://trac.openturns.org`.

Soize, C. (2000). A nonparametric model of random uncertainties for reduced matrix models in structural dynamics. *Probabilistic Engineering Mechanics 15*(3), 277–294.